Available online at www.sciencedirect.com
SCIENCE DIRECT
Biochemical Pharmacology 70 (2005) 481–488
Biochemical Pharmacology
www.elsevier.com/locate/biochempharm

Depletion of RLIP76 sensitizes lung cancer cells to doxorubicin

Sharad S. Singhal [a], Sushma Yadav [a], Jyotsana Singhal [a], Ewa Zajac [a], Yogesh C. Awasthi [b], Sanjay Awasthi [a,*]

[a] Department of Chemistry and Biochemistry, University of Texas at Arlington, Arlington, TX 76019-0065, USA
[b] Department of Human Biological Chemistry and Genetics, University of Texas Medical Branch at Galveston, Galveston, TX 77555-0645, USA

Received 9 December 2004; accepted 4 May 2005

Abstract

Ral-interacting protein (RLIP76) (RALBP1) is an anti-apoptotic non-ABC glutathione (GSH)-conjugate transporter involved in receptor-ligand endocytosis, as well as in multispecific drug transport and resistance. Partial inhibition of RLIP76 using antibodies in the absence of chemotherapy drug causes apoptosis in multiple small cell lung cancer (SCLC) and non-small cell lung cancer (NSCLC) cell lines and in the presence of doxorubicin (DOX), marked synergy is observed. These findings indicated that RLIP76 should be a good target for cancer cell killing; its down-regulation would promote apoptosis through both drug-dependent and drug-independent effects. To examine the effect of complete and specific RLIP76 depletion on apoptosis, we tested the effects of RLIP76 siRNA in a number of lung cancer cell lines. Growth inhibition and apoptosis was observed in all cases upon RLIP76 depletion. Consistent with these findings, augmenting cellular RLIP76 through transfection or liposomal protein delivery conferred resistance to apoptosis mediated by either DOX or 4-hydroxynonenal (4-HNE). Taken together, our results show that RLIP76 is rational and promising new target for lung cancer therapy.

Keywords: Transfection; siRNA; Doxorubicin; Drug-resistance; RLIP76; RALBP1

1. Introduction

The era of proteomics and genomics has resulted in identification of a plethora of potential targets for development as small molecule drugs and numerous nominally targeted lead compounds await demonstration of efficacy and clinical relevance [1]. Limited resources dictate that highly selected targets with established clear rationale can be considered initially for further development. Since chemotherapy remains a mainstay of therapy for unresectable as well as many resectable cancers, apoptosis and the major mechanism for chemotherapy drug action, it is logical to consider drug-resistance and apoptosis pathway proteins as preferred targets. Ral-interacting protein (RLIP76) (RALBP1) fulfils this criterion quite well. It is a novel link between glutathione (GSH) linked oxidant defenses, phase I and II biotransformation, stress-signaling, receptor-ligand pair endocytosis and the Ral and Rac-1 signaling pathways [2–10].

RLIP76 was cloned as a Ral-binding protein and predicted to be an effector involved in regulation of membrane plasticity, movement and endocytosis [9–11]. We have identified RLIP76 as a highly active efflux mechanisms for removing glutathione-electrophile conjugate (GS-E, i.e. LTC_4) from cells [12]. It represents the predominant GS-E transporter in lung cancer cells [6,12–16]. In addition to GS-E, the exceptionally broad substrate specificity of RLIP76 extends to anthracycline and vinca alkaloids, towards which it mediates resistance [4–6,8,12–16]. Its mechanism of action appears to be through interaction with the membrane by antennapedia-homeodomain homologous sequences within the N-terminal, coupled with ATP-hydrolysis simulated by substrate binding [14]. In membranes, it is localized, bound to clathrin through clathrin adaptor protein2 (AP2) [17] and partner of RALBP1/RLIP76 (POB1) [18], which is phosphorylated

Abbreviations: DNP-*S*G, dinitrophenyl *S*-glutathione; DOX, doxorubicin; GS-E, glutathione-electrophile conjugate; GSH, glutathione; 4HNE, 4-hydroxynonenal; MRP, multi-drug resistance associated protein; NSCLC, non-small cell lung cancer; POB1, partner of RLIP76; RLIP76 (RALBP1), Ral-interacting protein; SCLC, small cell lung cancer; TUNEL, TdT-mediated dUTP nick end labeling

* Corresponding author. Tel.: +1 817 272 5444; fax: +1 817 272 3808.
E-mail address: sawasthi@uta.edu (S. Awasthi).

0006-2952/$ – see front matter © 2005 Elsevier Inc. All rights reserved.
doi:10.1016/j.bcp.2005.05.005

by EGF-receptor in a complex with epsin and Grb-2 [19]. Our recent findings show that POB1 is an inhibitor of the GS-E transport function of RLIP76, in context of studies by others showing inhibition of growth factor signaling [18,20] and induction of apoptosis by POB1, strongly indicate that the GS-E transport activity of RLIP76 plays a key role in diverse membrane functions, one of which is the efflux of structurally unrelated xenobiotics and their metabolites. Our recent studies of gene-disruption of RLIP76 (mouse homolog designated RIP1) in mice confirm this assertion, showing that RLIP76 homozygous knockout mice have >80% loss of GS-E transport activity in tissues and are very sensitive to the toxic effects of X-irradiation [21].

In previous studies, we have shown that inhibition of RLIP76 by anti-RLIP76 antibodies induced apoptosis in the absence of DOX and synergistically enhanced doxorubicin (DOX) cytotoxicity through increased cellular accumulation of DOX [7]. These studies were consistent with previous results in which RLIP76-mediated increased cellular GS-E transport activity and oxidant-stress-resistance was abrogated by anti-RLIP76 antibodies which caused apoptosis due to increase in the endogenous lipid-peroxidation derived alkylating agent, 4-hydroxynonenal [2]. Because these effects could be confounded by direct effects of antibodies on the clathrin-coated pit mediated endocytosis, we carried out present studies to examine more directly the effects of specific depletion of RLIP76 by siRNA and, conversely, of augmenting RLIP76 by either transfection or direct liposomal delivery. Results of our studies show that RLIP76 depletion acutely induces apoptosis and that augmentation of RLIP76 protects from the cytotoxicity of DOX through increased DOX-efflux and decreased cellular DOX-accumulation.

2. Materials and methods

2.1. Materials

Sources of reagents were the same as previously described [4,8]. Human small cell lung cancer (SCLC) lines, H182, H1618 and non-small cell lung cancer (NSCLC) lines H226 and H520 (squamous cell carcinoma), H1395 and H2347 (adenocarcinoma), H2126 (large cell) and H358 (bronchioalveolar) were a kind gift from Dr. Adi F. Gazdar at U.T. Southwestern Medical Center, Dallas, Texas. All cells were cultured at 37 °C in a humidified atmosphere of 5% CO_2 in RPMI-1640 medium supplemented with 10% (v/v) heat-inactivated FBS, 1% (v/v) P/S solution, 2 mM L-glutamine, 10 mM HEPES, 1 mM sodium pyruvate, 4.5 g/L glucose and 1.5 g/L sodium bicarbonate. Viable cell density was determined using trypan blue-exclusion in a hemocytometer.

2.2. Cell cultures and drug sensitivity

2×10^4 Cells were plated into each well of 96-well microtiter plate 24 h prior to addition of medium containing varying concentrations of DOX or 4-hydroxynonenal (4HNE). MTT assay was carried out 96 h later as previously described [22] with eight replicate wells per measurement and three separate experiments to determine IC_{50}. Measured absorbance values were directly linked with a spreadsheet for calculation of IC_{50}, defined as the DOX concentration that reduced formazan formation by 50%. For determination of the effect of augmenting RLIP76 by liposomes, cells were incubated with medium containing RLIP76 liposomes or control liposomes (prepared in the absence of RLIP76) for 24 h prior to addition of drug. For determination of the effect of RLIP76 depletion using siRNA, cells were incubated for 3 h with 2 μg/well RLIP76 siRNA in Transmessenger Transfection Reagent (Qiagen). Cells were then washed with PBS, followed by 24–96 h incubation at 37 °C in medium before MTT assay.

2.3. Stable transfection of RLIP76 in SCLC and NSCLC cells

H1618 (SCLC) and H358 (NSCLC) were transfected with the eukaryotic expression vector alone (pcDNA-3.1) or with pcDNA3.1-RLIP76 as previously described for K562 cells [4]. Stable transfectants selected in presence of 600 μg/ml G418 and maintained in medium containing 300 μg/ml G418. Single clonal stable transfectants was established by sequential dilution into 96-well plate, such that only a single cell was seeded in each well. Expression of RLIP76 mRNA in lung cancer cell lines was evaluated by RT-PCR analysis. The RNA prepared by RNeasy kit (Qiagen) was quantified and 2 μg RNA was subjected to 1% agarose gel electrophoresis in MOPS-formaldehyde buffer for 3 h at 50 V. RLIP76 gene-specific primers [1228–1245 bp (upstream primer) and 1948–1968 bp (downstream primer)] were used for RT-PCR. Levels of MRP1, MRP3 and MRP5 were also determined by RT-PCR in the vector and RLIP76 transfected clones as well as untransfected controls. MRP1 (ABCC1) gene-specific primers [4117–4136 bp (upstream primer) and 4603–4620 bp (downstream primer)], MRP3 (ABCC3) gene-specific primers [3602–3621 bp (upstream primer) and 4413–4432 bp (downstream primer)], MRP5 (ABCC5) gene-specific primers [3783–3802 bp (upstream primer) and 4109–4128 bp (downstream primer)] were used. Ready-to-go RT-PCR beads were used according to the manufacturer's instructions (Amersham Biosciences). Levels of RLIP76 protein in control and transfected clones were measured by immunoassay using anti-RLIP76 IgG. Aliquots of crude detergent membrane fraction of cells containing 100 μg protein were applied to SDS-PAGE and Western blot analyses was performed according to the method of Towbin et al. [23].

Purified recombinant human RLIP76 with purity assessed by amino acid composition analysis was used to generate calibration curves to convert scanning densitometry data to microgram protein. RLIP76 protein content was measured as previously reported in homogenates prepared from 2×10^6 cells of each type by an ELISA assay (Sigma) using anti-RLIP76 IgG.

2.4. Transport studies in crude membrane vesicles

Crude membrane inside-out vesicles were prepared from membrane fraction of cell lines [8] and transport studies of DOX and dinitrophenyl *S*-glutathione (DNP-*S*G) in crude membrane vesicles were performed by the method described previously [4,8]. ATP-dependent uptake of 14-[^{14}C]-DOX (specific activity 8.5×10^4 cpm/nmol) or ^{3}H-DNP-SG (specific activity 3.9×10^3 cpm/nmol) was determined by subtracting the radioactivity of the control without ATP from that of the experimental containing ATP and the transport of DOX or DNP-SG was calculated in terms of pmol/(min mg^{-1}) protein.

2.5. Effect of RLIP76 liposomes on ^{14}C-DOX accumulations in lung cancer cells

The SCLC and NSCLC cells lines were harvested, washed with PBS and aliquots containing 5×10^6 cells (in triplicate) were inoculated into fresh medium. After overnight incubation, the cells were pelleted and resuspended in 50 μl medium containing 10 μg RLIP76 liposomes or control liposomes and incubated at 37 °C for 24 h. After 24 h incubation, 14-[^{14}C]-DOX (3.6 μM) was then added to the medium and incubated for additional 20 min at 37 °C. Cells were centrifuged at 4 °C and medium was completely decanted and washed the cell pellet twice with PBS. Radioactivity was determined in the cell pellet.

2.6. RLIP76 siRNA preparation

We chose aa 171–185 (nucleotide 510–555 starting from 1 AUG codon in the open reading frame) in the N-terminal region of RLIP76 as the target region to design for siRNA because of lack of homology with other proteins or nucleotide sequences. We searched for 23-nucleotide sequence motif, AA(N19)TT or NA(N21) (N, any nucleotide) and selected hits with approximately 50% GC contents. The sequence of sense siRNA corresponds to N21. We converted 3′ end of the sense siRNA to TT. The rationale for this sequence conversion was to generate a symmetric duplex with respect to the sequence composition of sense and antisense 3′ overhangs. The antisense siRNA was synthesized as the complement to position 1–21 of the 23-nucleotide motif. The selected siRNA sequence was blast-search (NCBI database) against EST libraries to ensure that only one gene is targeted. Chemically synthesized siRNA duplex in the 2′ de-protected and desalted forms was purchased from Dharmacon Research (Lafayette, CO). A 23-nucleotide long scrambled siRNA duplex was used as a control. The scrambled siRNA sequence was not homologous with RLIP76 mRNA in a blast-search against RLIP76. The siRNA duplex was resuspended in 1× universal buffer, provided by Dharmacon Research Laboratory. The targeted cDNA sequence (AAGAAAAAGCCAATTCAGGAGCC) corresponds to aa 170–176 (nt 508–528). The corresponding sense and antisense siRNA sequences are GAAAAAGCCAAUUCAGGAGCCdTdT and GGCUCCUGAAUUGGCUUUUUCdTdT, respectively. The sequence of the scrambled siRNA in the sense and antisense directions are GUAACUGCAACGAUUUCGAUGdTdT and CAUCGAAAUCGUUGCAGUUACdTdT, respectively. Transfection of siRNA duplexes was performed using Transmessenger Transfection Reagent kit (Qiagen) and assay for silencing 24 h after transfection.

2.7. Effect of RLIP76 siRNA on apoptosis by TUNEL assays

For NSCLC cells, aliquots of cells (1×10^6 cells) were placed into 12-well plates containing coverslips. After 24 h incubation with medium, coverslips were incubated with RLIP76 or control siRNA in Transmessenger Transfection Reagent for 3 h. Excess siRNA was washed off with PBS and medium was added. For SCLC, which grows in suspension, 1×10^6 cells were placed into 12-well plates and allowed to grow for 24 h. Cells were suspended into medium and transferred to eppendorf tubes and incubated with control or RLIP76 siRNA in Transmessenger Transfection Reagent for 3 h. After 24 h incubation, TdT-mediated dUTP nick end labeling (TUNEL) assay was performed using Promega Fluorescence Detection kit. Fluorescence photomicrographs were taken using a Zeiss LSM510 META (Germany) laser scanning fluorescence microscope at 400× magnification.

3. Results

3.1. Effect of depleting cellular RLIP76

siRNA mediated down-regulation of RLIP76 was developed through sequence analyses of RLIP76, focusing on sequences unique to RLIP76 and those conducive for use as siRNA. Of multiple candidate siRNA, the most effective down-regulation of RLIP76 was found for siRNA-16, corresponding to nt 508–528. A progressive, time-dependent decrease in RLIP76 protein was seen by Western blot analyses in cells treated with siRNA-16, but not from the corresponding scrambled siRNA control (Fig. 1A). At 24 and 48 h after siRNA treatment, RLIP76 was undetectable by Western blot analyses. We have previously shown that anti-RLIP76 antibodies caused increased accumulation of

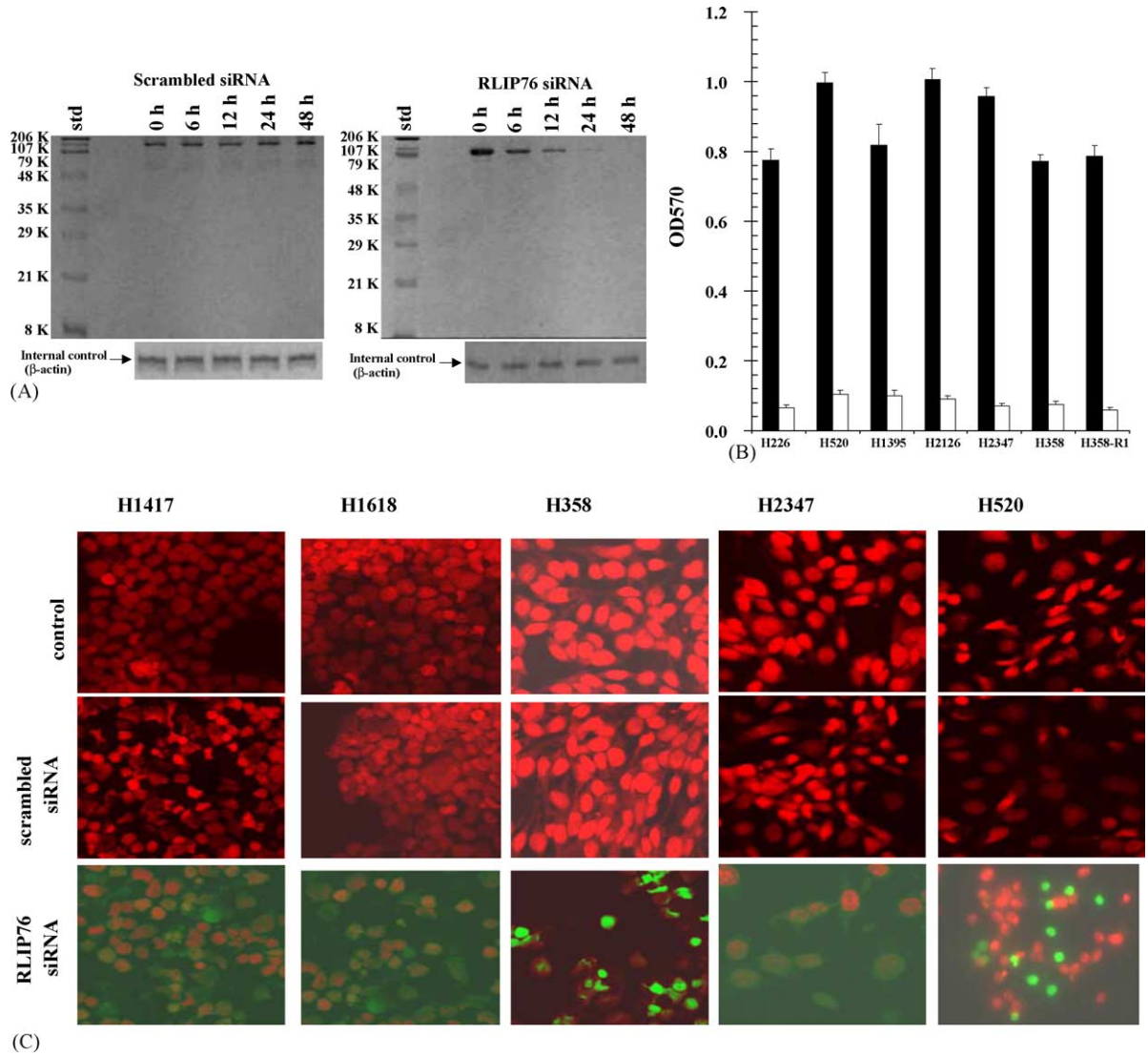

Fig. 1. (A) Depletion of RLIP76 by siRNA and its effects on cell survival by MTT and on apoptosis by TUNEL assay in lung cancer cells RLIP76 siRNA directed at nt 508–528 or a scrambled control was transfected into lung cancer cell lines using Transmessenger Transfection Reagent (Qiagen). The time-dependent effect of RLIP76 siRNA (2 μg/well) were evaluated using the H358 NSCLC cell line by determining RLIP76 protein levels using Western blot analyses at 0, 6, 12, 24 and 48 h after treatment of RLIP76 siRNA. β-Actin was used as an internal control. (B) MTT assay in the H226, H358, H520, H1395, H2126, H2347 and H358-R1 (RLIP76 transfected clone) performed 48 h after treatment of siRNA: scrambled siRNA (black bars) and RLIP76 siRNA (white bars). (C) Induction of apoptosis is shown for the H1417, H1618, H358, H2347 and H520 cell lines using a TUNEL assay in which green fluorescence represent apoptotic cells.

the pro-apoptotic oxidative lipid metabolite, 4HNE and caused apoptosis within 48 h after exposure to several lung cancer cell lines in the absence of any chemotherapy agent [7]. Those findings led us to propose that depletion of RLIP76 transport activity, with resultant accumulation of 4HNE, resulted in apoptosis. Since the present siRNA was very effective at depleting RLIP76, we evaluated its effect on cell survival by MTT assay at varying concentration of the siRNA in six NSCLC cell lines (Fig. 1B) as well as in the H358-R1 RLIP76 overexpressing clone, where ~90% loss of cell viability was observed within 48 h after exposure to RLIP76 siRNA at a concentration of 2 μg/well. To determine whether this effect was due to triggering of apoptosis as we have previously demonstrated in six NSCLC cell lines with anti-RLIP76 antibodies, we performed a TUNEL fluorescence apoptosis assay. Results of these studies presented for the H358, H2347 and H520 NSCLC and H1618 and H1417 SCLC cell lines (Fig. 1C) clearly demonstrated apoptosis caused by the RLIP76 siRNA, the scrambled control siRNA had no effect. Taken together, these results conclusively demonstrate that specific depletion of RLIP76 acutely triggers apoptosis in lung cancer cells and indicate a new avenue for targeted anti-neoplastic therapy of lung cancer.

3.2. The effect of augmenting cellular RLIP76

Since depletion of RLIP76 triggers apoptosis, increasing it in cell should confer resistance to apoptosis induced by DOX. We tested this hypothesis by examining the effect of

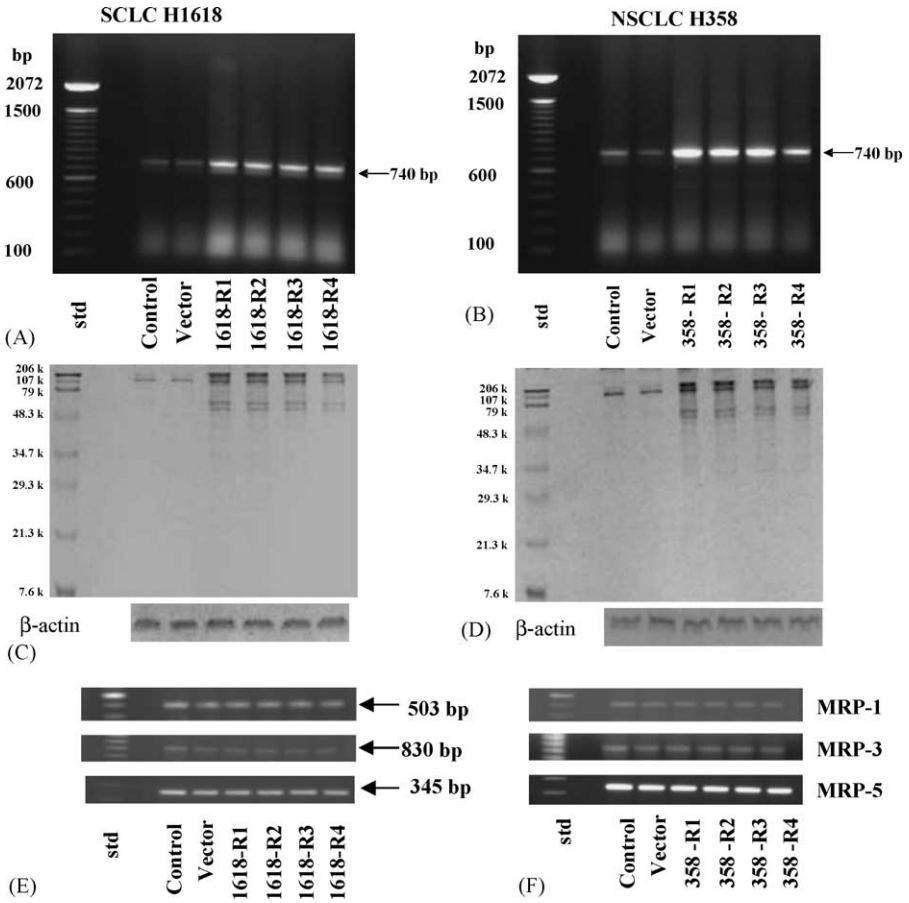

Fig. 2. Transfection of RLIP76 in SCLC and NSCLC H1618 (SCLC, panels A, C and E) and H358 (NSCLC, panels B, D and F) were transfected with the eukaryotic expression vector alone (pcDNA-3.1) or with pcDNA3.1-RLIP76 using Effectene Transfection Reagent kit (Qiagen). Four stable clonal transfectants (R1–R4) were chosen for studies. Expression of RLIP76 mRNA in lung cancer cell lines was evaluated by RT-PCR analysis (panels A and B) and fold induction of RLIP76 was checked by densitometry of the 740 bp band. RNA was prepared by RNeasy kit (Qiagen) and RT-PCR was performed using RLIP76 gene-specific primers [1228–1245 bp (upstream primer) and 1948–1968 bp (downstream primer)]. Comparisons of RLIP76 protein levels were performed in Western blot analysis (panels C and D). Hundred micrograms aliquots of crude membrane extracts were applied to SDS-PAGE and Western blotting against RLIP76 IgG. Scanning densitometry was used to measure the sum of intensities of the bands at 109 and 67 kDa, former being intact full-length RLIP76 with actual molecular mass of 76.1 kDa by MALDI-MS [9,12] and the latter a splice/alternative start site variant beginning at Met203 [37]. β-Actin was used as an internal control. Expression of MRP1 (ABCC1), MRP3 (ABCC3) and MRP5 (ABCC5) was evaluated by RT-PCR using MRP1, -3 and -5 gene-specific primers as described in Section 2 (panels E and F).

augmenting RLIP76 expression through stable transfection or using liposomal delivery on cellular DOX-accumulation, -efflux and -resistance. Four transfected clones each from H1618-SCLC and H358-NSCLC cell lines were randomly selected after transfection with RLIP76-pcDNA-3.1 using lipofectin. Three- to five-fold increase in RLIP76 mRNA was confirmed in both H1618 and H358 using RT-PCR (Fig. 2A and B). Western blot analysis against anti-RLIP76-IgG on detergent extracts of crude membrane fraction of these clones revealed an approximately four-fold increase in RLIP76 expression in both H1618 and H358 (Fig. 2C and D). The expression levels of MRP1 (ABCC1), MRP3 (ABCC3) and MRP5 (ABCC5) were unaffected by RLIP76 transfection in all transfectants of both H1618 and H358 (Fig. 2E and F). The accumulation of DOX compared by incubating cells with 14-[^{14}C]-DOX for 30 min and determining uptake in the cell pellet was higher (4.0 ± 0.2-fold) in wild-type or vector-alone transfected cells as compared to cell transfected with RLIP76 (Table 1). Comparison of ATP-dependent transport of DOX and DNP-*S*G transport rates in crude membrane vesicles demonstrated a clearly increased transport rate in all four clones from both H1618 and H358. RLIP76 overexpressing clones from both H1618 SCLC and H358 NSCLC were significantly more resistant to both DOX and 4HNE. Taken together, these findings show that stable transfection of RLIP76 confers transport mediated resistance to DOX and to the endogenous alkylating agent, 4HNE.

Because forced overexpression of RLIP76 could lead to multiple compensatory genetic alterations and potentially confound the results of such studies in stable transfectants, we utilized an alternative method for increasing cellular RLIP76, through the use of RLIP76 liposomes as a delivery vehicle. Recombinant human RLIP76 was purified to homogeneity as previously described and reconstituted

Table 1
Effects of augmenting RLIP76 on transport and cytotoxic sensitivity in lung cancer cells[a]

Method for augmenting RLIP76	Cell line	Fold change as compared with control						
		RLIP76-mRNA	RLIP76 protein	Cellular DOX uptake	DOX-transport	DNP-*SG* transport	4HNE sensitivity	DOX resistance
Transfection	H1618-V	1.0 ± 0.1	1.0 ± 0.1	1.0 ± 0.1	1.0 ± 0.0	1.5 ± 0.4	1.0 ± 01	1.0 ± 0.1
	H1618-R1	4.9 ± 0.4	4.9 ± 0.7	0.23 ± 0.02	4.7 ± 0.4	6.5 ± 1.0	3.3 ± 0.1	4.8 ± 0.6
	H1618-R2	4.9 ± 0.3	4.6 ± 0.6	0.26 ± 0.04	4.4 ± 0.5	6.1 ± 0.3	2.8 ± 0.1	4.4 ± 0.6
	H1618-R3	4.1 ± 0.5	4.7 ± 0.7	0.27 ± 0.02	3.8 ± 0.2	5.9 ± 0.5	2.5 ± 0.1	4.1 ± 1.1
	H1618-R4	4.4 ± 0.4	4.0 ± 0.6	0.24 ± 0.04	4.5 ± 0.4	6.0 ± 0.9	2.7 ± 0.1	4.3 ± 0.7
	H358-V	0.8 ± 0.1	0.9 ± 0.1	1.0 ± 0.01	1.0 ± 0.03	0.9 ± 0.04	0.9 ± 0.1	1.0 ± 0.2
	H358-R1	4.4 ± 0.2	3.8 ± 0.5	0.24 ± 0.02	5.5 ± 0.4	7.4 ± 0.6	3.2 ± 0.1	5.2 ± 0.8
	H358-R2	4.3 ± 0.5	3.8 ± 0.5	0.23 ± 0.03	4.8 ± 0.6	6.8 ± 0.8	2.7 ± 0.1	4.1 ± 0.4
	H358-R3	4.2 ± 0.4	3.1 ± 0.4	0.25 ± 0.03	4.9 ± 0.7	6.8 ± 0.3	2.7 ± 0.1	4.2 ± 0.6
	H358-R4	2.8 ± 0.1	3.2 ± 0.4	0.24 ± 0.04	4.6 ± 0.6	5.2 ± 0.4	2.1 ± 0.1	3.1 ± 0.4
RLIP76-Liposomal Delivery	H182	–	3.5 ± 0.3	0.25 ± 0.02	–	–	–	2.9 ± 0.2
	H1618	–	3.6 ± 0.4	0.28 ± 0.04	–	–	–	3.8 ± 0.3
	H226	–	4.2 ± 0.8	0.27 ± 0.05	–	–	–	4.1 ± 0.4
	H2347	–	4.5 ± 0.9	0.31 ± 0.04	–	–	–	3.8 ± 0.3

[a] Cellular content of RLIP76 was augmented in H1618 or H358 by stable transfection. V-designates vector-alone transfection and R1–R4 are four independent clones of each cell line. mRNA content was quantified by densitometric quantitation of RT-PCR performed as described in the legends for Fig. 2. RLIP76 protein was quantified by ELISA assay utilizing a kit from Sigma and anti-RLIP76 IgG; standard curves were prepared using purified recombinant RLIP76. DOX uptake by intact cells was measured as described in Section 2. DOX and DNP-*SG* transport was performed in crude membrane inside-out vesicles prepared from cell membranes of each cell line. An MTT-cytotoxicity assay was performed to determine the sensitivity to 4HNE and DOX. Average and standard deviations from three separate experiments are presented. Each transport study was performed with three replicates and each cytotoxicity study with eight replicates. As compared with vector transfected controls, values for RLIP76 transfectants were significant at $p < 0.01$ by the Student's *t*-test for all data presented.

into artificial liposomes [4]. Cells were incubated with medium containing 50 μg purified RLIP76 protein/mL liposomes for 24 h, followed by washing four times with PBS. The cells were pelleted, washed twice and RLIP76 was quantified in the cell pellet as well as the last wash-supernatant by ELISA assay standardized for RLIP76. While the RLIP76 level in the wash-supernatant from cells treated with either control liposomes was below the detectable limit, the cells treated with RLIP76 liposomes had 3.9 ± 0.9-fold higher RLIP76 level ($n = 4$, two SCLC and two NSCLC cell lines) as compared with cells treated with control liposomes (Table 1), achieved without genetic manipulation. DOX uptake in SCLC was only 1.6-fold higher ($P < 0.05$) than in NSCLC, despite the approximately 10-fold greater IC_{50} of NSCLC as compared with SCLC. Concomitant with the nearly four-fold increase in RLIP76 level, the uptake of DOX decreased to nearly 1/4 (28 ± 2%) of that observed in cells treated with control liposomes (Table 1). The two native SCLC cell lines were an order of magnitude more sensitive to DOX than the two native NSCLC cell lines, an expected finding (Table 1). RLIP76 liposome treated SCLC as well as NSCLC cell lines with approximately 4-fold augmented RLIP76 levels after treatment with RLIP76 liposomes were significantly more resistant to DOX (3.7 ± 0.5-fold, $n = 4$ with two SCLC and two NSCLC cell lines) than control liposome treated cells in which RLIP76 level was unchanged from untreated controls. Taken together, these findings show that RLIP76 liposomes can be used to deliver RLIP76 to lung cancer cells and that this results in a marked decrease in cellular DOX-accumulation along with significantly increased DOX-resistance.

4. Discussion

Present studies, in which specific depletion of RLIP76 using siRNA caused apoptosis in all lung cancer cell lines tested, combined with results showing that RLIP76 transfection confers increased GS-E transport as well as 4HNE-resistance, strongly support the conclusion that a physiological function of RLIP76 is to inhibit apoptosis signaling by controlling intracellular levels of pro-apoptotic endogenous lipid-peroxidation byproducts by catalyzing the efflux of their GS-E. 4HNE (and other alkenals) alone trigger apoptosis [3,24–31] and inhibition of RLIP76 has been shown to increase cellular accumulation of 4HNE [2,32]. However, other potential RLIP76-mediated mechanisms for inhibition of apoptosis could be postulated. 4HNE is a model alkenal, but by no means the only one, and lipid-derived glutathione conjugates are not limited to alkenals. RLIP76 is a multifunctional protein, which has been shown to exhibit GAP activity (inhibition) towards cdc42. Activation of cdc42, a Rho family G-protein, has been shown to induce apoptosis [33]. Expression of wild-type or a constitutively active mutant of Cdc42 results in caspase activation and apoptosis, whereas expression of a dominant-negative mutant of Cdc42 diminishes p53-dependent apoptosis [34]. If the GAP activity and transport activity of RLIP76 are viewed as competing activities, conditions which lead to increased cellular GS-E would result in a greater fraction of RLIP76 bound to GS-E and functioning in transport, thus releasing inhibition of cdc42. A sudden overwhelming increase in GS-E, as would occur if the major efflux mechanism were suddenly blocked, would tilt the balance towards GS-E

transport and away from cdc42-GAP activity. Conversely, an increase in GS-E results in inhibition of GST resulting in increased accumulation of the electrophilic lipid-peroxidation products (such as alkenals and epoxides), which are sufficiently stable to diffuse into the nucleus and sufficiently reactive to form DNA-aducts and mediate apoptosis though a p53-dependent mechanism. This may be sufficient to trigger apoptosis though JNK. It should be noted that either inhibition of RLIP76 [2,3] or activation of cdc42 [34,35] has been shown to initiate JNK signaling.

Recent studies have shown that overexpression of POB1 (partner of RALBP1, an RLIP76-binding protein) triggers apoptosis in prostate cancer cells [18]. We have recently shown that POB1 is a specific inhibitor of the transport of DOX and GS-E by RLIP76 and have shown that augmenting POB1 triggers apoptosis, in the absence of any chemotherapy drug, in lung cancer cells as well. Inhibition of cellular RLIP76 by increasing POB1 also resulted in increased accumulation and decreased efflux of DOX, as well as significant sensitization to DOX [36]. Present studies examining the converse, the effect of increased cellular RLIP76, clearly show that it is capable of directly affecting cellular DOX-accumulation, -efflux and -resistance. These findings strongly support the assertion that RLIP76 is a GS-E transporter, which because of its broad substrate specificity also functions as a drug transporter. Its inhibition in the absence of drug, either by antibodies [7] or siRNA, triggers apoptosis; its inhibition in the presence of drug confers synergistic increase in cytotoxicity of DOX [7] as well as vinorelbine [13]. The direct involvement of RLIP76 in apoptosis as well as drug-transport mediated resistance suggests that it should be an excellent candidate for targeting inhibitors to improve the efficacy of GS-E forming drugs (i.e. platinum coordinates) and natural product drugs (i.e. vinorelbine).

Acknowledgements

Supported in part by NIH grants CA 77495 and CA 104661(SA), ES 012171 (YCA) and Cancer Research Foundation of North Texas (SA). We thank Dr. Sophia Passy and Chad Larson, Biology Department, University of Texas at Arlington, Arlington, TX, for helping and providing Confocal Laser Microscope and LSM Image Analysis software, supported by the National Science Foundation Grant 0215852.

References

[1] Workman P. The opportunities and challenges of personalized genome-based molecular therapies for cancer: targets, technologies, and molecular chaperones. Cancer Chemother Pharmacol 2004;52:S45–56.

[2] Cheng JZ, Sharma R, Yang Y, Singhal SS, Sharma A, Saini MK, et al. Accelerated metabolism and exclusion of 4-hydroxynonenal through induction of RLIP76 and hGST5.8 is an early adaptive response of cells to heat and oxidative stress. J Biol Chem 2001;276:41213–23.

[3] Yang Y, Sharma A, Sharma R, Patrick B, Singhal SS, Zimniak P, et al. Cells preconditioned with mild, transient UVA irradiation acquire resistance to oxidative stress and UVA-induced apoptosis: role of 4-hydroxynonenal in UVA-mediated signaling for apoptosis. J Biol Chem 2003;278:41380–8.

[4] Awasthi S, Cheng J, Singhal SS, Saini MK, Pandya U, Pikula S, et al. Novel function of human RLIP76: ATP-dependent transport of glutathione conjugates and doxorubicin. Biochemistry 2000;39:9327–34.

[5] Awasthi S, Cheng JZ, Singhal SS, Pandya U, Sharma R, Singh SV, et al. Functional reassembly of ATP-dependent xenobiotic transport by the N- and C-terminal domains of RLIP76 and identification of ATP binding sequences. Biochemistry 2001;40:4159–68.

[6] Awasthi S, Singhal SS, Singhal J, Cheng J, Zimniak P, Awasthi YC. Role of RLIP76 in lung cancer doxorubicin resistance II. Doxorubicin transport in lung cancer by RLIP76. Int J Oncol 2003;22:713–20.

[7] Awasthi S, Singhal SS, Singhal J, Yang Y, Zimniak P, Awasthi YC. Role of RLIP76 in lung cancer doxorubicin resistance III. Anti-RLIP76 antibodies trigger apoptosis in lung cancer cells and synergistically increase doxorubicin cytotoxicity. Int J Oncol 2003;22:721–32.

[8] Awasthi S, Singhal SS, Srivastava SK, Zimniak P, Bajpai KK, Saxena M, et al. Adenosine triphosphate-dependent transport of doxorubicin, daunomycin, and vinblastine in human tissues by a mechanism distinct from the P-glycoprotein. J Clin Invest 1994;93:958–65.

[9] Jullien-Flores V, Dorseuil O, Romero F, Letourneur F, Saragosti S, Berger R, et al. Bridging Ral GTPase to Rho pathways. RLIP76, a Ral effector with CDC42/Rac GTPase-activating protein activity. J Biol Chem 1995;270:22473–7.

[10] Morinaka K, Koyama S, Nakashima S, Hinoi T, Okawa K, Iwamatsu A, et al. Epsin binds to the EH domain of POB1 and regulates receptor-mediated endocytosis. Oncogene 1999;18:5915–22.

[11] Rosse C, Hoste S, Offner N, Picar A, Camonis J. RLIP an effector of the Ral GTPases, is a platform for cdk1 to phosphorylate epsin during switch off of endocytosis in mitosis. J Biol Chem 2003;278:30597–604.

[12] Sharma R, Singhal SS, Wickramarachchi D, Awasthi YC, Awasthi S. RLIP76 (RALBP1)-mediated transport of leukotriene C4 (LTC_4) in cancer cells: implications in drug resistance. Int J Cancer 2004;112:934–42.

[13] Stuckler D, Singhal J, Singhal SS, Yadav S, Awasthi YC, Awasthi S. RLIP76 transports vinorelbine and mediates drug resistance in non-small cell lung cancer. Cancer Res 2005;65:991–8.

[14] Yadav S, Singhal SS, Singhal J, Wickramarachchi D, Knutson E, Albrecht TB, et al. Identification of membrane anchoring domains of RLIP76 using deletion mutants analyses. Biochemistry 2004;43:16243–53.

[15] Awasthi S, Sharma R, Singhal SS, Zimniak P, Awasthi YC. RLIP76, a novel transporter catalyzing ATP-dependent efflux of xenobiotics. Drug Metab Dispos 2002;30:1300–10.

[16] Awasthi S, Singhal SS, Sharma R, Zimniak P, Awasthi YC. Transport of glutathione-conjugates and chemotherapeutic drugs by RLIP76 (RLIP76): a novel link between G-protein and tyrosine kinase signaling and drug resistance. Int J Cancer 2003;106:635–46.

[17] Jullien-Flores V, Mahe Y, Mirey G, Leprince C, Meunier-Bisceuil B, Sorkin A, et al. RLIP76, an effector of the GTPase Ral, interacts with AP2 complex: involvement of the Ral pathway in receptor endocytosis. J Cell Sci 2000;113:2837–44.

[18] Oosterhoff J, Penninkhof KF, Brinkmann AO, Grootegoed JA, Blok LJ. REPS2/POB1 is downregulated during human prostate cancer progression and inhibits growth factor signaling in prostate cancer cells. Oncogene 2003;22:2920–5.

[19] Kariya K, Koyama S, Nakashima S, Oshiro T, Morinaka K, kikuchi A. Regulation of complex formation of POB1/epsin/adaptor protein complex 2 by mitotic phosphorylation. J Biol Chem 2000;275:18399–406.

[20] Penninkof F, Grrotegoed JA, Blok LJ. Identification of REPS2 as a putative modulator of NF-κB activity in prostate cancer cells. Oncogene 2004;23:5607–15.
[21] Awasthi S, Singhal SS, Yadav S, Singhal J, Drake K, Nadkar A, et al. RLIP76 is a major determinant of radiation sensitivity. Cancer Res 2005, in press.
[22] Awasthi S, Sharma R, Singhal SS, Chaubey M, Herzog NK, Awasthi YC. Sulfasalazine enhances the cytotoxicity of cisplatin towards human small cell lung cancer cell lines. Br J Cancer 1994;70: 190–4.
[23] Towbin H, Staehelin T, Gordon J. Electrophoretic transfer of protein from polyacrylamide gels to nitrocellulose sheets: procedure and some applications. Proc Natl Acad Sci 1979;76:4350–3.
[24] Zhang W, He Q, Chan LL, Zhou F, El Naghy M, Thompson EB, et al. Involvement of caspases in 4-hydroxy-alkenal-induced apoptosis in human leukemic cells. Free Rad Biol Med 2001;30:699–706.
[25] Choudhary S, Zhang W, Zhou F, Campbell GA, Chan LL, Thompson EB, et al. Cellular lipid peroxidation end-products induce apoptosis in human lens epithelial cells.. Free Rad Biol Med 2002;32:360–9.
[26] Cheng JZ, Singhal SS, Saini M, Singhal J, Piper JT, Van Kujik FJ, et al. Effects of mGSTA4 transfection on 4-hydroxynonenal-mediated apoptosis and differentiation of K562 human erythroleukemia cells. Arch Biochem Biophys 1999;372:29–36.
[27] Cheng JZ, Singhal SS, Sharma A, Saini M, Yang Y, Awasthi S, et al. Transfection of mGSTA4 in HL-60 cells protects against 4-hydroxynonenal-induced apoptosis by inhibiting JNK-mediated signaling. Arch Biochem Biophys 2001;392:197–207.
[28] Sharma R, Brown D, Awasthi S, Yang Y, Sharma A, Patrick B, et al. Transfection with 4-hydroxynonenal-metabolizing glutathione *S*-transferase isozymes leads to phenotypic transformation and immortalization of adherent cells. Eur J Biochem 2004;271:1690–701.
[29] Camandola S, Poli G, Mattson MP. The lipid peroxidation product 4-hydroxy-2,3-nonenal increases AP-1 binding activity through caspase activation in neurons. Neurochemistry 2000;74:159–68.
[30] Soh Y, Jeong KS, Lee IJ, Bae MA, Kim YC, Song BJ. Selective activation of the c-Jun N-erminal protein kinase pathway during 4-hydroxynonenal-induced apoptosis of PC 12 cells. Mol Pharmacol 2000;58:535–41.
[31] Liu W, Kato M, Akhand AA, Hayakawa A, Suzuki H, Miyata T, et al. 4-Hydroxynonenal induces a cellular redox status-related activation of the caspase cascade for apoptotic cell death. Cell Sci 2000;113: 635–41.
[32] Awasthi YC, Yang Y, Tiwari NK, Patrick B, Sharma A, Li J, et al. Regulation of 4-hydroxynonenal-mediated signaling by glutathione *S*-transferases. Free Rad Biol Med 2004;37:607–19.
[33] Su J-L, Lin M-T, Hong C-C, Chang C-C, Shiah S-G, Wu C-W, et al. Resveratrol induces FasL-related apoptosis through Cdc42 activation of ASK1/JNK-dependent signaling pathway in human leukemia HL-60 cells. Carcinogenesis 2005;1:1–10.
[34] Thomas A, Giesler T, White E. p53 mediates bcl-2 phosphorylation and apoptosis via activation of the Cdc42/JNK1 pathway. Oncogene 2000;19:5259–69.
[35] Lee YN, Malbon CC, Wang HY. G alpha 13 signals via p1 15RhoGEF cascades regulating JNK1 and primitive endoderm formation. J Biol Chem 2004;279:54896–904.
[36] Yadav S, Zajac E, Singhal SS, Singhal J, Drake K, Awasthi YC, et al. POB1 over-expression inhibits RLIP76-mediated transport of glutathione-conjugates, drugs and promotes apoptosis. Biochem Biophys Res Commun 2005;328:1003–9.
[37] Quaroni A, Paul EC. Cytocentrin is a Ral-binding protein involved in the assembly and function of the mitotic apparatus. J Cell Sci 1999;112:707–18.